Influence of the Bite Angle on the Hydroformylation of Internal Olefins to Linear Aldehydes

Raymond P. J. Bronger, Paul C. J. Kamer, and Piet W. N. M. van Leeuwen*

Institute of Molecular Chemistry, University of Amsterdam, Nieuwe Achtergracht 166, 1018 WV Amsterdam, The Netherlands

Received July 2, 2003

A novel series of ligands (**1**−**10**) that induce wide bite angles (106° < β_n < 131°) has been synthesized. Compared to the xantphos series (e.g., **13** versus **5**), the introduction of the phosphacyclic moiety results in ligands with a slightly larger bite angle. High-pressure IR and high-pressure NMR studies of the (diphosphine)$RhH(CO)_2$ complexes show that most ligands (**3**−**7**) adopt a bis-equatorial binding mode exclusively in the trigonal bipyramidal rhodium complex. Subtle changes in ligand structure have a large impact on activity and selectivity in the hydroformylation of 1-octene and *trans*-2-octene. Rates up to 3275 (mol aldehyde)(mol Rh)$^{-1}$ h^{-1} ($p(CO/H_2)$ = 20 bar, T = 353 K, [Rh] = 1 mM, [1-octene] = 637 mM) and regioselectivities > 99% toward the linear product were obtained when 1-octene was used as substrate. For *trans*-2-octene rates up to 250 (mol aldehyde)(mol Rh)$^{-1}$ h^{-1} ($p(CO/H_2)$ = 3.6 bar, T = 393 K, [Rh] = 1 mM, [*trans*-2-octene] = 640 mM) and high regioselectivities up to 96% toward the linear product, which are unprecedented, were obtained. A correlation between the selectivity for the hydroformylation of 1-octene and *trans*-2-octene has been observed, suggesting that the selectivity-determining step remains unchanged between terminal and internal olefins. Ligands with a larger bite angle lead to more selective systems, but above 125° the regioselectivity drops. Furthermore it is no longer the selective formation of linear alkyl species that determines the high regioselectivities. Instead the differences in rate of β-hydrogen elimination from the branched alkyl intermediate and the linear alkyl intermediate versus CO insertion determine the regioselectivity. For both substrates a *decrease* in activity with an *increase* in bite angle is observed. It is suggested that the aforementioned rates of β-hydrogen elimination versus CO insertion must play a crucial role in this bite angle effect on activity, because previous studies have shown that an *increase* in bite angle leads to an *increase* in activity.

Introduction

To date, the hydroformylation reaction is one of the most important homogeneously catalyzed reactions in the world, covering an annual production of almost eight million tons of aldehydes and alcohols, from which butanal and 2-ethylhexanol are the most important products.[1,2] Nowadays, the design of new ligands and systematic tuning of their electronic and steric properties are common research topics in this area, as it provides insight in regio- and chemoselectivity and the overall catalytic activity.[3−11] Tolman introduced the cone angle θ and the electronic parameter χ to classify phosphorus ligands with respect to their steric bulk and phosphine basicity.[12] Both parameters have been used extensively as a measure of ligand properties in hydroformylation studies.[13,14] Casey and Whiteker developed the concept of natural bite angle (the P−M−P angle) as an additional characteristic of diphosphine ligands to rationalize the correlation found between the regioselectivity and the coordination mode of bidentate ligands possessing wide bite angles.[5] Many articles and reviews have appeared that discuss the effect of the bite angle on activity and selectivity for a number of catalytic reactions.[15−20] The bite angle induces not only steric effects but also electronic effects, as the P−M−P angles

* Corresponding author. E-mail: pwnm@science.uva.nl.

(1) Weissermel, K.; Arpe, H.-J *Industrielle Organische Chemie*; VCH Verlagsgesellschaft mbH: Weinheim, 1988.
(2) *Rhodium Catalyzed Hydroformylation*; van Leeuwen, P. W. N. M., Claver, C., Eds.; Kluwer Academics Publishers: Dordrecht, 2000.
(3) van der Veen, L. A.; Boele, M. D. K.; Bregman, F. R.; Kamer, P. C. J.; van Leeuwen, P. W. N. M.; Goubitz, K.; Fraanje, J.; Schenk, H.; Bo, C. *J. Am. Chem. Soc.* **1998**, *120*, 11616−11626.
(4) van der Veen, L. A.; Keeven, P. H.; Schoemaker, G. C.; Reek, J. N. H.; Kamer, P. C. J.; van Leeuwen, P. W. N. M.; Lutz, M.; Spek, A. L. *Organometallics* **2000**, *19*, 872−883.
(5) Casey, C. P.; Whiteker, G. T. *Isr. J. Chem.* **1990**, *30*, 299−304.
(6) Casey, C. P.; Paulsen, E. L.; Beuttenmueller, E. W.; Proft, B. R.; Petrovich, L. M.; Matter, B. A.; Powell, D. R. *J. Am. Chem. Soc.* **1997**, *119*, 11817−11825.
(7) Casey, C. P.; Paulsen, E. L.; Beuttenmueller, E. W.; Proft, B. R.; Matter, B. A.; Powell, D. R. *J. Am. Chem. Soc.* **1999**, *121*, 63−70.
(8) Klein, H.; Jackstell, R.; Wiese, K.-D.; Borgmann, C.; Beller, M. *Angew. Chem., Int. Ed. Commun.* **2001**, *40*, 3408−3411.
(9) Selent, D.; Hess, D.; Wiese, K. D.; Rottger, D.; Kunze, C.; Borner, A. *Angew. Chem., Int. Ed.* **2001**, *40*, 1696−1698.
(10) van der Veen, L. A.; Kamer, P. C. J.; van Leeuwen, P. W. N. M. *Organometallics* **1999**, *18*, 4765−4777.
(11) Kranenburg, M.; van der Burgt, Y. E. M.; Kamer, P. C. J.; van Leeuwen, P. W. N. M. *Organometallics* **1995**, *14*, 3081.
(12) Tolman, C. A. *Chem. Rev.* **1977**, *77*, 313−348.
(13) Moser, W. R.; Papile, C. J.; Brannon, D. A.; Duwell, R. A.; Weininger, S. J. *J. Mol. Catal.* **1987**, *41*, 271−292.
(14) van Leeuwen, P. W. N. M.; Roobeek, C. F. *J. Organomet. Chem.* **1983**, *258*, 343−350.
(15) Dierkes, P.; van Leeuwen, P. W. N. M. *J. Chem. Soc., Dalton Trans.* **1999**, 1519−1529.

10.1021/om034012f CCC: $25.00
Publication on Web 11/11/2003

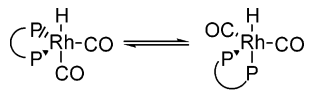

ee **ae**

Figure 1. ee−ae equilibrium in rhodium trigonal bipyramidal complexes.

clearly affect the nature of the complex or intermediate states. In a review by Freixa and van Leeuwen an attempt is made to separate the contributions of the *steric bite angle effect* and the *electronic bite angle effect* to the selectivities and rates for several catalytic reactions, including hydroformylation.[16] For hydroformylation it was first believed that the coordination mode of the diphosphine in the (diphosphine)$RhH(CO)_2$ complex, either equatorial−equatorial (ee) or apical−equatorial (ae) (Figure 1), was a key factor in controlling the regioselectivity of the hydroformylation reaction. Later studies by van Leeuwen et al.[3] showed that the coordination mode is not the sole factor determining the outcome of the reaction.

It has been reported that phosphacyclic derivatives of different ligands with the right backbone, e.g., ligands based on 2,2′-dimethylbisphenyl, and xanthene backbones, like cyclic phosphines,[10,21] cyclic phosphites,[9,22−24] cyclic phosphonites,[25] and cyclic phosphorus diamides,[26] result in catalysts that show a high activity and selectivity for the hydroformylation of terminal olefins. Especially the catalytic activity is enhanced considerably compared to noncyclic analogues. Decreased phosphorus basicity and increased electron "elasticity", which is attributed to the extended conjugation of the ligand π-system, are considered to be the main reasons for this observed effect.[4,10,13,27]

Generally terminal olefins are used as substrates, while from an economical point of view internal olefins or a mixture of internal olefins and terminal olefins are substrates of choice, yet linear aldehydes and alcohols are the preferred products. To obtain linear aldehydes from internal olefins, the system has to catalyze isomerization between the internal and terminal olefin, as the thermodynamic mixture contains in general less than 5% of the terminal olefin. In addition the hydroformylation of the terminal olefin must be many times faster than the hydroformylation of the internal olefin. Also, a high selectivity toward the linear aldehyde is required. Nevertheless, catalysts that fulfill all these requirements are not per se good catalysts for the hydroformylation of internal olefins to linear aldehydes.[28] Although considerable progress in this field has been made by the use of bulky phosphites[22,24,29] and phosphonites,[25] these systems suffer from a low long-term stability due to alcoholysis, hydrolysis, and thermal instability.[30,31] Phosphines are more resistant to these degradation reactions, but afford in general less active catalysts. To date, only few rhodium-diphosphine systems are known that show a respectable activity and selectivity for the hydroformylation of internal olefins. Van Leeuwen et al. introduced phenoxaphosphino- and dibenzophosphole-modified xanthene ligands (**11** and **12**, Figure 2),[10,21] while Beller et al. introduced Naphos-type ligands with various electron-withdrawing substituents (Figure 3).[8]

Recently, the effect of natural bite angle on the catalytic activity and selectivity on the hydroformylation of terminal olefins was investigated, for which a series of diphosphine ligands with different xanthene-type backbones was prepared.[4,11] These ligands, however, are not suitable for a study of the bite angle effect on the hydroformylation of internal alkenes to linear aldehydes, as the rate of isomerization from the internal olefin to the terminal olefin is too low to ensure fast and selective catalysis. Xanthene-type ligands bearing phosphacyclic moieties do give systems that are suitable for the hydroformylation of internal alkenes.[10,21] To obtain a better understanding of how the bite angle affects the hydroformylation activity and selectivity of internal olefins, we synthesized a range of phenoxaphosphino-modified xanthene-type ligands that show a regular increase in natural bite angle (Figure 3, ligands **1**−**8**). In addition, two new dibenzophosphole xanthene-type ligands have been synthesized (**9** and **10**) to obtain a better insight into the effect of ligand backbone and other phosphacyclic moieties. The coordination chemistry and the performance in the rhodium-catalyzed hydroformylation of 1-octene and *trans*-2-octene for this novel series of ligands will be described. Furthermore, deuterioformylation reactions of 1-hexene with ligands **1**, **5**, and **7** were performed. The number and position of the deuterium atoms that are incorporated in the aldehyde and isomerized hexenes give detailed information about the reversibility of the different reaction steps during hydroformylation.[28,32−35]

Results

Synthesis. A total of 10 novel ligands that are closely related in either backbone structures or phosphine

(16) Freixa, Z.; van Leeuwen, P. W. N. M. *J. Chem. Soc., Dalton Trans.* **2003**, 1890−1901.
(17) Kamer, P. C. J.; Reek, J. N. H.; van Leeuwen, P. W. N. M. *Chemtech* **1998**, 27−33.
(18) Kamer, P. C. J.; van Leeuwen, P. W. N. M.; Reek, J. N. H. *Acc. Chem. Res.* **2001**, *34*, 895.
(19) van Leeuwen, P. W. N. M.; Kamer, P. C. J.; Reek, J. N. H.; Dierkes, P. *Chem. Rev.* **2000**, *100*, 2741.
(20) van Leeuwen, P. W. N. M.; Kamer, P. C. J.; van der Veen, L. A.; Reek, J. N. H. *Chin. J. Chem.* **2001**, *19*, 1−8.
(21) van der Veen, L. A.; Kamer, P. C. J.; van Leeuwen, P. W. N. M. *Angew. Chem., Int. Ed.* **1999**, *38*, 336−338.
(22) Billig, E.; Abatjoglou, A. G.; Bryant, D. R.; Murray, R. E.; Maher, J. M. (Union Carbide Corp.) Eur. Pat. Appl. EP 213,639, 1987.
(23) Billig, E.; Abatjoglou, A. G.; Bryant, D. R.; Murray, R. E.; Maher, J. M. U.S. Pat. US 4,717,775, 1988.
(24) Dieleman, C. B.; Kamer, P. C. J.; Reek, J. N. H.; van Leeuwen, P. W. N. M. *Helv. Chim. Acta* **2001**, *84*, 3269−3279.
(25) Selent, D.; Wiese, K.-D.; Rottger, D.; Borner, A. *Angew. Chem., Int. Ed.* **2000**, *39*, 1639−1641.
(26) van der Slot, S. C.; Kamer, P. C. J.; van Leeuwen, P. W. N. M.; Fraanje, J.; Goubitz, K.; Lutz, M.; Spek, A. L. *Organometallics* **2000**, *19*, 2504−2515.
(27) Hayashi, T.; Tanaka, M.; Ogata, I. *J. Mol. Catal.* **2003**, *6*, 1−9.
(28) van der Slot, S. C.; Duran, J.; Luten, J.; Kamer, P. C. J.; van Leeuwen, P. W. N. M. *Organometallics* **2002**, *21*, 3873−3883.
(29) Burke, P. M.; Garner, J. M.; Tam, W.; Kreutzer, K. A.; Teunissen, A. J. J. M.; Snijder, C. S.; Hansen, C. B. (DSM/Du Pont de Nemours) WO97/33854, 1997.
(30) Kamer, P. C. J.; Reek, J. N. H.; van Leeuwen, P. W. N. M. Rhodium Phosphite Catalysts. In *Rhodium Catalyzed Hydroformylation*; van Leeuwen, P. W. N. M., Claver, C., Eds.; Kluwer Academic Publishers: Dordrecht, 2000; pp 35−62.
(31) van Leeuwen, P. W. N. M. *Appl. Catal. A* **2001**, *212*, 61−81.
(32) Casey, C. P.; Petrovich, L. M. *J. Am. Chem. Soc.* **1995**, *117*, 6007−6014.
(33) Lazzaroni, R.; Settambolo, R.; Raffaelli, A.; Pucci, S.; Vitulli, G. *J. Organomet. Chem.* **1988**, *339*, 357−365.
(34) Lazzaroni, R.; Uccello-Barretta, G.; Benetti, M. *Organometallics* **1989**, *8*, 2323−2327.
(35) Consiglio, G.; Morandini, F.; Haelg, P.; Pino, P. *J. Mol. Catal.* **1990**, *60*, 363−374.

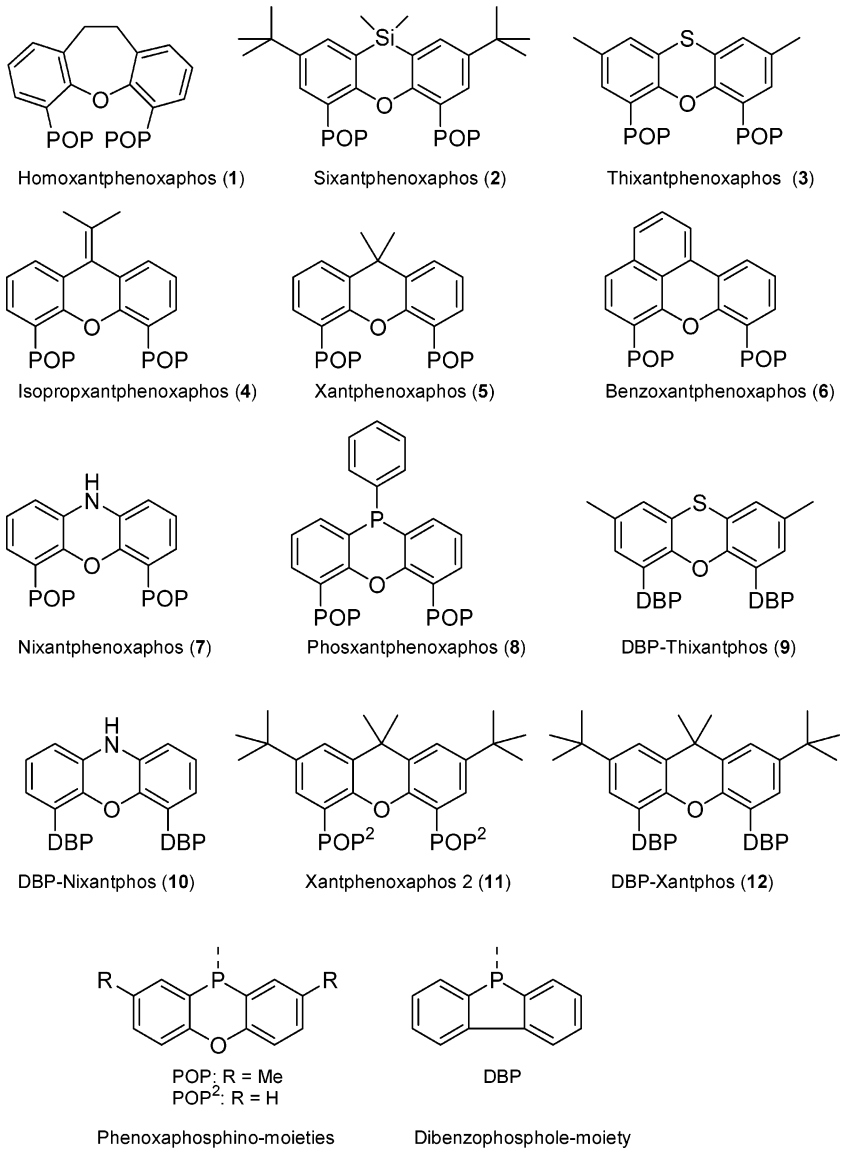

Figure 2. Phosphacyclic xanthene type ligands. **11** and **12** were reported previously.[10,21]

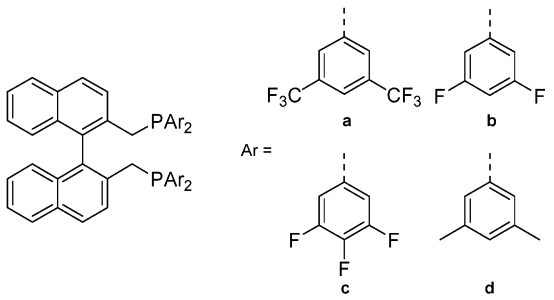

Figure 3. Naphos-type ligands suitable for hydroformylation of internal alkenes.

Scheme 1. Synthesis of Ligands 1−10[a]

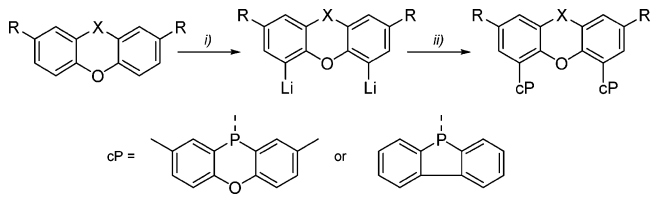

[a] (*i*) *n*-BuLi, TMEDA, 0 °C, (*ii*) chlorophosphine, −78 °C.

moieties were synthesized (**1**−**10**). The ligand backbones were prepared according to literature procedures or were commercially available. Selective dilithiation of the backbones followed by the reaction with the chlorophosphine yields the corresponding ligands in moderate to high yields (30−80%) (Scheme 1). Accidentally, in $^{31}P\{^{1}H\}$ NMR no distinction between the two different phosphorus signals of **6** could be made, but they lose their degeneracy in the (**6**)$Rh(CO)_2H$ complex.

Ligands with the phenoxazine backbone (**7** and **10**) were obtained via a slightly modified procedure. The secondary amine functionality of phenoxazine was protected using chloro-*tert*-butyldimethylsilane. Lithiation of the protected backbone followed by the reaction with the chlorophosphine and subsequent deprotection gave the ligands in moderate yields after crystallization (30%−43%). For the synthesis of **8** phenyllithium instead of *n*-butyllithium was used as metallating agent in order to prevent side product formation by nucleophilic substitution of the phenyl of the phosphine by *n*-butyllithium.

Molecular mechanics calculations of ligands **1**−**10** show the effect of the heterocycle on the calculated natural bite angle and the flexibility range (Table 1).[5] The calculations show that the rigid 2,8-dimethylphen-

Table 1. Calculated Natural Bite Angles and Flexibility Ranges for the Phenoxaphosphino-Modified Xantphos-Type Ligands

ligand	backbone	β_n[a] (deg)	flexibility range[a] (deg)
1	10,11-dihydrodibenzo[*b*,*f*]oxepine	105.7	91−128
2	2,7-di-*tert*-butyl-10,10-dimethylphenoxasilin	108.0	106−137
3	2,7-dimethylphenoxathiin	112.5	107−140
4	10-isopropylidenexanthene	114.2	110−144
5	9,9-dimethylxanthene	116.0	100−134
6	benzo[*k*,*l*]xanthene	124.3	117−156
7	phenoxazine	124.5	113−151
8	10-phenylphenoxaphosphine	131.2	126−153
9	2,7-dimethylphenoxathiin	111.8	98−133
10	phenoxazine	128.9	117−145
11[b]	2,7-di-*tert*-butyl-9,9-dimethylxanthene	123.1	107−142
12[b]	2,7-di-*tert*-butyl-9,9-dimethylxanthene	121.4	107−138

[a] The natural bite angle (β_n) and the flexibility range were calculated as by Casey and Whiteker. β_n is defined as the preferred chelation angle determined only by backbone constraints and not by metal valence angles. The flexibility range is defined as the accessible range of bite angles within 3 kcal mol^{-1} excess strain energy from the calculated natural bite angle. [b] See also refs 10, 21.

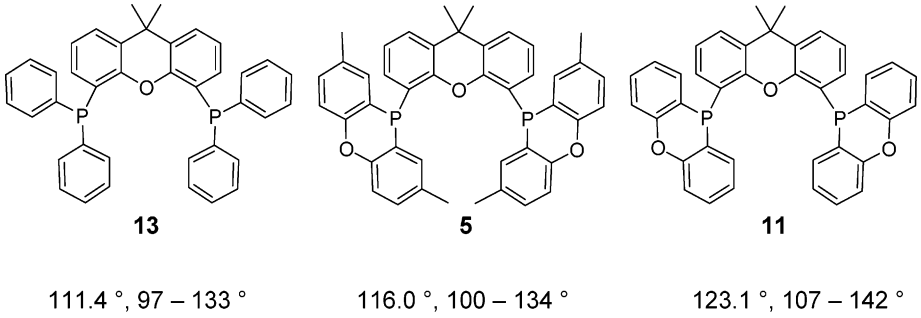

Figure 4. Effect of phosphine moiety on bite angle and flexibility range (β_n, flexibility range).

oxaphosphino moiety causes an increase of the bite angle compared to the corresponding diphenylphosphino analogues, while the introduction of the methyl substituents on the phenoxaphosphino moiety causes a decrease in bite angle compared to the unsubstituted phenoxaphosphine (Figure 4). Ligand **8** has a calculated natural bite angle that is much wider than expected from the ligand backbone structure, as calculations performed on the diphenylphosphino analogue show a much smaller bite angle. In the case of **8** the phenyl substituent in the backbone structure is in close proximity of one of the methyl substituents on each phenoxaphosphino moiety, thereby forcing the phenoxaphosphino moieties to adopt a different orientation from that initially expected, which results in an increased bite angle.

(Diphosphine)Rh(CO)$_2$H Complexes. To determine whether the variation in ligand backbone has an influence on the chelation behavior of the ligands, we studied the solution structures of the (diphosphine)Rh(CO)$_2$H complexes, the resting state of the catalyst under hydroformylation conditions, by high-pressure IR and high-pressure NMR spectroscopy. The complexes were prepared in situ from Rh(CO)$_2$(acac) and diphosphine (1.1 equiv) under 16 bar of CO/H$_2$ (1:1). For ligands **1**−**8** the formation of (diphosphine)Rh(CO)$_2$H was observed to occur within 1 h at 40 °C. The ^{31}P{^{1}H} NMR spectrum at 273 K of the complexes with **2**−**5**, **7**, and **8** showed a characteristic doublet in the range from −33 to −20 ppm. For ligands **1**, **9**, and **10** [(diphosphine)Rh(CO)$_2$]$_2$ were observed as the major complexes. These dimers exhibit a splitting pattern in ^{31}P{^{1}H} NMR consistent with an AA′A″A‴XX′ spin system at − 27.4 ppm for **1**, 4.8 ppm for **9**, and −0.4 ppm for **10**.[36]

Table 2. Selected High-Pressure NMR Data for (Diphosphine)RhH(CO)$_2$ Complexes[a]

ligand	^1J(Rh,H), Hz	^1J(Rh,P), Hz	$^2J_{av}$(P,H), Hz	^2J(P,P), Hz	δ^{31}P{^{1}H} (ppm)	δ^1H (ppm)
1	11.9	124/129	42		−20.4	−8.9
2	n.o.[b]	150	6.6		−23.7	−8.7
3	2.9	153	12.4		−25.3	−8.9
4	2.8	154	12.5		−27.2	−9.0
5	n.o.	151	7.7		−29.0	−9.0
6[c]	n.o.	153/149	6.6	63	−33.0	−9.2
7[d]	n.o.	153	13.5		−30.8	−9.2
8	n.o.	153	bs		−25.7	−8.9

[a] Conditions: p(CO/H$_2$)(1:1) = 20 bar, solvent = toluene-d_8, T = 273 K. [b] n.o.: not observed. [c] Solvent = toluene-d_8/THF. [d] Solvent = THF-d_8.

The complex (**1**)Rh(CO)$_2$H was observed in lower quantities, showing two broad doublets, indicating mainly ae coordination. (**9**−**10**)Rh(CO)$_2$H were not observed at all. For (**6**)Rh(CO)$_2$H a double doublet per phosphorus atom was observed due to the inequivalence of the two phosphorus atoms. In the ^{1}H NMR at 273 K the hydride appeared in the range from −9.2 to −8.7 ppm as a triplet of doublets for ligands **1**, **3**, and **4**, a triplet for **2** and **5**−**7**, or a broad (distorted) singlet for **8**. The characteristic heteronuclear coupling constants and chemical shifts are shown in Table 2.

Probably due to the high concentration that is required for high-pressure NMR, often small amounts of additional rhodium-phosphine species were observed. Both ^{1}H NMR and ^{31}P{^{1}H} NMR using ^{13}CO exclude these species as either hydride- or carbonyl-containing complexes. For ligand **8** many other phosphorus−rhodium species, besides formation of (**8**)Rh(CO)$_2$H, are

(36) Castellanos-Paez, A.; Castillon, S.; Claver, C.; van Leeuwen, P. W. N. M.; de Lange, W. G. J. *Organometallics* **1998**, *17*, 2543−2552.

Table 3. Selected High-Pressure IR Data for (Diphosphine)RhH(CO)$_2$ Complexes[a]

ligand	ν_1[b]	ν_2[b]	ν_3[b]	ν_4[b]
1	2040	1999	1978	1956
2	2041	2000(vw)	1981	1953(vw)
3	2042		1985	
4[c]	2037		1979	
5	2040		1983	
6[c]	2036		1979	
7	2040		1984	
8[c]	2038	2004	1980	1954

[a] Conditions: $p(CO/H_2)(1:1) = 20$ bar, solvent = cyclohexane, $T = 313$ K. [b] Vibrational bands belonging to either the ee or ae configuration were assigned by performing a H−D exchange. [c] Solvent = 2-methyltetrahydrofuran.

observed in considerable amounts in $^{31}P\{^1H\}$ NMR. The relatively high concentration of ligand and rhodium that is necessary for high-pressure NMR when compared to the conditions of a catalytic reaction is a plausible cause for the observation of so many species in which coordination of the additional phosphine of the ligand backbone can be involved. The disappearance of the signal of the free phosphorus of the ligand backbone at −53 ppm indicates that this phosphorus atom is indeed coordinating, reinforcing this hypothesis. The distorted broad signal at −8.9 ppm in ^1H NMR might be the result of two overlapping signals, which would indicate the presence of more than one rhodium-hydride species. Even at 183 K the signals could not be separated. Formation of telomeric, oligomeric, or polymeric structures is not excluded. Characterization of the different species has not been attempted.

The IR frequencies of the absorption bands of the (**1**−**8**)Rh(CO)$_2$H complexes in the carbonyl region are summarized in Table 3. For the rhodium complexes with ligands **3**−**7** only two absorption bands were observed. By performing a hydride−deuterium exchange the two bands shifted to a lower frequency. This indicates that the ligands are coordinated in an ee fashion, as in this isomer a trans relationship between the hydride and carbonyl ligand exists, which results in coupling of the vibrations. By exchange of H for D this resonance interaction becomes much smaller, which leads to a shift of the carbonyl bands of the ee isomer.[3] Only when ligands **1**, **2**, and **8** were used was the existence of an equilibrium between ee and ae coordinating rhodium complexes observed, as complexes with these ligands showed all four absorption bands in the carbonyl frequency region. Unlike the high-pressure NMR experiments, no formation of the dimeric [(**1**)Rh(CO)$_2$]$_2$ was observed. This is ascribed to the low concentrations that are used for high-pressure IR and which are similar to those of catalytic runs, while high-pressure NMR needs much higher concentrations, which favors the formation of dimeric rhodium species.

For **10** only the dimeric complex [(**10**)Rh(CO)$_2$]$_2$ was observed in the IR spectrum. This complex exhibits absorption bands for the terminal carbonyl ligands (2004 cm^{-1}/1980 cm^{-1}) and two absorption bands in the bridging carbonyl ligands (1792 cm^{-1}/1762 cm^{-1}). Similar dimeric complexes were also observed for **12**.[10,21] [(**12**)Rh(CO)$_2$]$_2$ was reported to be the resting state of the catalyst. For **9** clearly other species were also formed. Besides two absorption bands for the terminal carbonyl ligands (2010 cm^{-1}/1985 cm^{-1}) and two absorption bands for the bridging carbonyl ligands (1801 cm^{-1}/1733 cm^{-1}), also absorptions at 2066 cm^{-1} (m) and 1994 cm^{-1} (s) were observed. In addition none of the CO bands shifted upon using D_2 instead of H_2. Clearly some other complexes are present when this ligand is used. This complex was not stable since the carbonyl absorptions diminished and many other absorptions with a low intensity appeared after overnight measurement at 80 °C.

Table 4. Hydroformylation of 1-Octene at 80 °C[a]

ligand	X[b]	β_n[b] (deg)	TOF[c,d]	l:b[c]	% isom[c]	sel[c,e]
1	C_2H_4	105.7	1900	5.5	2.8	82
2	$Si(CH_3)_2$	108.0	2250	14	6.8	87
3	S	112.5	3275	22	10.5	85
4	isoprop	114.2	1800	23	9.7	86
5	$C(CH_3)_2$	116.0	1800	23	10.0	86
6	fused ring	124.3	1600	30	12.5	84
7	NH	124.5	1550	33	11.6	85
8	PPh	131.2	1100	18	7.5	87
9	S	111.8	343	>99	14.2	85
10	NH	128.9	144	>99	11.5	87
11	$C(CH_3)_2$	123.1	1557	67	10.0	89
12	$C(CH_3)_2$	121.4	453	62	10.8	88

[a] Conditions: $p(CO/H_2)(1:1) = 20$ bar, ligand/Rh = 5, substrate/Rh = 637, [Rh] = 1.00 mM in toluene, number of experiments is 3. In none of the experiments was hydrogenation observed. [b] X = refers to the top bridging group in the ligand (see Figure 2); β_n = the natural bite angle (see Table 1). [c] Linear over branched ratio, percent linear aldehyde, percent isomerization to 2-octene, and turnover frequency were determined at ∼ 20% alkene conversion. [d] Turnover frequency = (mol aldehyde)·(mol Rh)$^{-1}$·h^{-1}. [e] Percentage of linear aldehyde of all products (including isomerization toward internal alkenes).

Hydroformylation of 1-Octene. Hydroformylation of 1-octene was carried out at 80 °C under 20 bar of 1:1 CO/H_2 using a 1.0 mM solution of rhodium diphosphine catalyst prepared from Rh(CO)$_2$(acac) and 5 equiv of ligand. The production of octene isomers, nonanal, and 2-methyloctanal was monitored by gas chromatography. Turnover frequencies were determined and averaged after ∼20% conversion. The results of the experiments are presented in Table 4.

In contrast to previous studies on the effect of bite angle on selectivity for the hydroformylation of 1-octene,[4] hardly any effect of the bite angle on the selectivity for the linear aldehyde is observed for ligands **1**−**8**. The l/b ratio and the percentage of isomerization to internal octenes increases, but both increase with increasing bite angle up to a bite angle of 125° only. The observed increase in l/b ratio is attributed to an increased tendency of the branched alkyl rhodium species to undergo β-hydrogen elimination instead of alkyl migration.[32] After an initial increase in catalytic activity with increasing bite angle from 105.7° up to 112.5° a drop in activity with further increasing bite angle is observed.

Ligand **3**, which according to the reported Hammet constant[37] has the strongest electron-withdrawing capacities with the sulfur moiety (σ_m(SPh) = 0.23[37]) in the ligand backbone, gives a catalytic system that shows almost twice the activity compared to the results obtained when the other phenoxaphosphino-modified ligands are employed. These results show that small structural and electronic differences can have a huge impact on catalysis results.

Very high regioselectivities and high percentages of isomerization are observed for the dibenzophosphole

(37) Hansch, C.; Leo, A.; Taft, W. *Chem. Rev.* **1991**, *91*, 165−195.

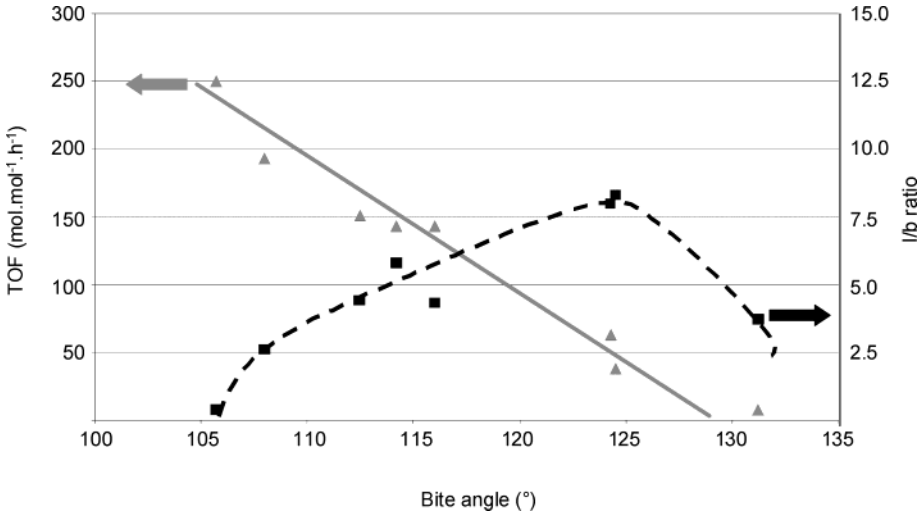

Figure 5. Turnover frequency (triangles) and regioselectivity (squares) vs the calculated natural bite angle in the hydroformylation of *trans*-2-octene (ligands **1**−**8**).

Table 5. Hydroformylation of *trans*-2-Octene at 120 °C[a]

ligand	X[b]	β_n[b] (deg)	TOF[c,d]	l:b[c]	sel[c,e]
1	C_2H_4	105.7	250	0.4	29
2	$Si(CH_3)_2$	108.0	193	2.6	72
3	S	112.5	151	4.4	81
4	isoprop	114.2	143	5.8	85
5	$C(CH_3)_2$	116.0	143	4.3	81
6	fused ring	124.3	63	8.0	89
7	NH	124.5	38	8.3	89
8	PPh	131.2	8	3.7	79
9	S	111.8	78 (64[f])	18.3 (22.7[f])	95 (96[f])
10	NH	128.9	60[f]	24.7[f]	96[f]
11	$C(CH_3)_2$	123.1	140 (112[f])	6.6 (9.2[f])	87 (90[f])
12	$C(CH_3)_2$	121.4	65[f]	9.5[f]	90[f]

[a] Conditions: $p(CO/H_2)(1:1) = 3.6$ bar, ligand/Rh = 10, substrate/Rh = 640, [Rh] = 1.00 mM in toluene, number of experiments is 2. In none of the experiments was hydrogenation observed. [b] X = refers to the top bridging group in the ligand (see Figure 2); β_n = the natural bite angle (see Table 1). [c] Linear over branched ratio, percent linear aldehyde, and turnover frequency were determined after 2 h. [d] Turnover frequency = (mol aldehyde)·(mol Rh)$^{-1}$·h^{-1}. [e] Percentage of linear aldehyde of all products other than octenes. [f] $p(CO/H_2)(1:1) = 2.0$ bar.

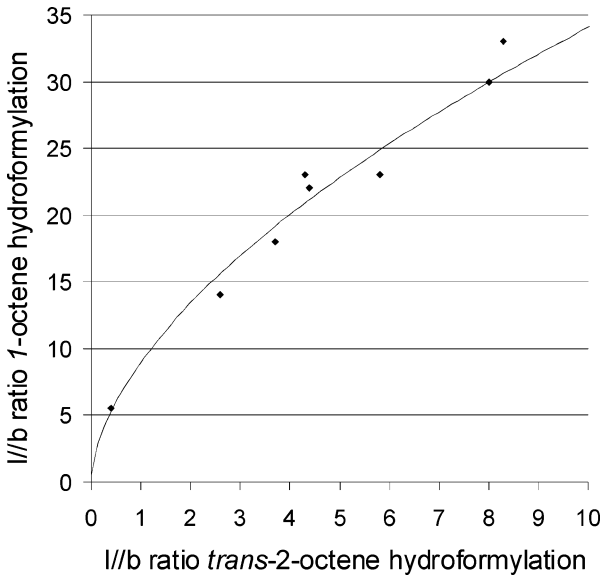

Figure 6. Parity plot 1-octene vs 2-octene hydroformylation with ligands **1**−**8**.

ligands **9** and **10**. For both ligands the hydroformylation activity is very low, but this can be a result of preferred formation of the rhodium-dimer resting state.

Hydroformylation of *trans*-2-Octene. Hydroformylation of *trans*-2-octene was carried out at 120 °C under 3.6 bar of 1:1 CO/H_2 using a 1.0 mM solution of rhodium diphosphine catalyst prepared from $Rh(PPh_3)_3H(CO)$ and 10 equiv of ligand. The relatively high temperature and low pressure are necessary to enhance the rate of isomerization,[38] thereby continuously maintaining the formation of terminal alkenes. The production of alkene isomers and linear and branched aldehydes was monitored by gas chromatography. Turnover frequencies were determined after 2 h reaction time.

The results of the hydroformylation experiments are summarized in Table 5.

By comparing ligands **1**−**8** a clear bite angle effect on catalytic activity and regioselectivity is observed in the hydroformylation of *trans*-2-octene; see Figure 5.

(38) van Rooy, A.; Orij, E. N.; Kamer, P. C. J.; van Leeuwen, P. W. N. M. *Organometallics* **1995**, *14*, 34−43.

Contrary to the results obtained with the noncyclic analogues for the hydroformylation of 1-octene,[4] an increased bite angle leads to a strong *decrease* in hydroformylation activity. While the activity decreases, an *increase* in regioselectivity is observed that correlates with the regioselectivity for the hydroformylation of 1-octene; see Figure 6 for a parity plot. As it is expected that the rate of isomerization is crucial for obtaining good catalysts for the selective hydroformylation of internal alkenes to linear aldehydes, it is not surprising that the ligands showing the highest rate of isomerization in the hydroformylation of 1-octene show the highest regioselectivity in the hydroformylation of *trans*-2-octene. In addition, ligands with a higher rate of isomerization show a lower hydroformylation activity, as β-hydrogen elimination is nonproductive.

Unprecedented high regioselectivities at moderate activities for the hydroformylation of *trans*-2-octene are obtained when the dibenzophoshole-type ligands **9** and **10** are used. These results can be attributed to the combination of the high isomerization activity and the

Table 6. Deuterioformylation of 1-Hexene[a]

ligand	conversion to aldehydes (%)	1-hexene (%)			2-hexene-d_1 (%)	heptanal-d_2 (%)[b]	2-methyl-hexanal-d_2 (%)[b]
		$CH_2{=}CHC_4H_9$	$CH_2{=}CDC_4H_9$	$CHD{=}CHC_4H_9$	$CHD\text{-}CH{=}CHC_3H_7$		
1	20.7	77.1	1.34	0.29	0.6	17.2	3.5
5	23.8	71.5	0.56	1.76	2.4	22.7	1.1
7	13.9	83.2	0.68	1.13	1.6	13.4	0.5

[a] Conditions: $p(CO/D_2) = 20$ bar ($\sim$ 1:1, see Experimental Section for more details), ligand/Rh = 5, substrate/Rh = 806, [Rh] = 1.00 mM in toluene. In none of the experiments was hydrogenation observed. It is important to note that the amounts of deuterated hexenes do not reflect the actual percentages of formed (1- and 2-alkyl)rhodium intermediates, as also nonproductive β-D elimination occurs. [b] Deuterium labels were almost exclusively found in the formyl group and the position β to the formyl group. Only traces of deuterium label was found at the position α to the formyl group.

Table 7. Partitioning of (Alkyl)rhodium Intermediates

ligand	(1-alkyl/2-alkyl) intermediate	l/b	(1-alkyl) intermediate[a]		(2-alkyl) intermediate[b]		
			heptanal (%)	$CH_2{=}CDC_4H_9$ (%)	2-methylhexanal (%)	$CDH{=}C_5H_{10}$ (%)	$CDH_2CH{=}C_4H_8$ (%)
1	4.22	4.9	92.8	7.2	79.7	6.6	13.7
5	4.42	20	97.6	2.4	20.9	33.5	45.6
7	4.37	25	95.2	4.8	15.5	35.0	49.5

[a] $CH_2{=}CDC_4H_9$ + heptanal = 100% (data converted from Table 6). [b] $CDH{=}C_5H_{10} + CDH_2CH{=}C_4H_8$ + 2-methylhexanal = 100% (data converted from Table 6).

very high regioselectivity of these ligands. Compared to ligands **1**−**8** only a small difference in hydroformylation activity between the 1-octene and *trans*-2-octene is observed, especially for **10**.

In an attempt to improve the regioselectivity even further, the effect of ligand concentration on activity and selectivity was investigated for **9**. Upon increasing the ligand:rhodium ratio from 5 to 40 equiv, a gradual decrease in TOF from 75 mol·mol^{-1}·h^{-1} to 34 mol·mol^{-1}·h^{-1} was observed. Within this range the regioselectivity did not change. This indicates a very strong coordination of the diphosphine to the rhodium metal; the formation of an inactive $(diphosphine)_2Rh$ species is favored at increased ligand:rhodium ratios.

Deuterioformylation of 1-Hexene. Deuterioformylation of 1-hexene was carried out under conditions similar to the hydroformylation experiments. 1-Hexene was used for the deuterioformylation instead of 1-octene to facilitate comparison with literature data of the ^1H and ^2H spectra.[32] The percentages of deuterated species formed in the deuterioformylation were calculated using GC and $^2H\{^1H\}$ NMR data on the ratio of heptanal to branched aldehydes, percent conversion, percent isomerization toward internal hexenes, and deuterium contents of aldehydes and recovered hexenes. Activities were comparable to the 1-octene hydroformylation experiments, while the regioselectivities are somewhat lower than those obtained with 1-octene. Table 6 summarizes the deuterioformylation results.

Previous studies by Casey,[32] Lazzaroni,[33,34] Pino,[35] and van Leeuwen[28] have shown that the formation of the alkylrhodium intermediate is reversible at elevated temperatures. By a similar experimental method, the amount of initial linear alkyl rhodium formation and branched alkyl rhodium formation can be easily deduced. Detailed dissection of the labeling results of catalysis with **1**, **5**, and **7** shows that the initial ratio of linear-alkyl to branched-alkyl intermediates is $\sim$4.2−4.4 (Table 7). These results prove that when these ligands are used, the differences in observed l/b ratio are not only the result of preferential formation of the linear aldehyde, but mainly the result of different rates of β-hydrogen elimination. In all three cases >92% of the linear alkyl intermediate reverts to the aldehyde directly. On the other hand, the branched alkyl intermediate partitions between conversion toward the branched aldehyde, 1-hexene, and *cis*- and *trans*-2-hexene.

From these results it can be concluded that increasing the bite angle in a branched alkyl rhodium intermediate causes a decrease in branched aldehyde formation, while the percentage of isomerization toward both 1-hexene and 2-hexene increases.

Discussion

Spectroscopy. The high-pressure NMR data of the (**1**−**8**)$RhH(CO)_2$ and [(**9**−**10**)$Rh(CO)_2$]$_2$ complexes are in line with the results obtained with high-pressure IR. For (**1**−**8**)$RhH(CO)_2$ the small rhodium−proton coupling constant and phosphorus−proton coupling constant and the large rhodium−phosphorus coupling constant indicate that the dynamic equilibrium between ee and ae isomers is shifted toward the ee isomer. Quantitative estimations of the ee:ae ratios for (**1**−**2**, **8**)$RhH(CO)_2$ cannot be made using the averaged phosphorus−proton coupling constants, as the ae and ee phosphorus−proton coupling constants are not known for these phosphacyclic diphosphines. As is indicated in Table 2, they can differ substantially between the different ligands; for example, a relatively large phosphorus−proton coupling is observed for complexes with ligands **3** and **7** and a small phosphorus−proton coupling is observed for the complex with ligand **2**. High-pressure IR indicates exclusive formation of ee isomers for the former two complexes and an ee−ae mixture for the latter complex. In nondisturbed trigonal bipyramidal complexes the phosphorus−hydride coupling should be very small;[4] therefore the results imply that in most cases the trigonal bipyramidal rhodium complexes are highly distorted, with the phosphines bent out of the equatorial plane. The rhodium−proton coupling constants are also indicative of the ee:ae ratio. The ae-coordinated isomers often have large rhodium−proton coupling constants, while for purely ee-coordinating ligands, like BISBI, small coupling constants are observed.[39] Moreover, in previous studies increasing ee:ae ratios were accompanied by decreasing rhodium−proton coupling con-

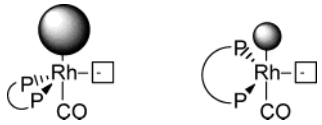

Figure 7. Effect of bite angle on space around rhodium.

stants.[3,4] It is surprising that for (**2**)$RhH(CO)_2$ the rhodium−proton coupling could not be resolved (^1J(Rh,H) < 2 Hz) even at low temperatures (183 K), while high-pressure IR clearly shows absorption bands belonging to the ae isomer, albeit in a small amount.

The results obtained by high-pressure IR suggest that the electron density around rhodium is similar for all (**1**−**8**)$RhH(CO)_2$ complexes, as all bands are within close range. Comparison of the CO-stretch frequencies with the (diphosphine)$RhH(CO)_2$ complexes of the diphenylphosphine analogues of ligands **1**−**8**[4] shows that all ligands have similar electronic properties. The large differences in catalytic activity between these two systems are therefore attributed to extended π-conjugation[21] and increased effective steric bulk upon introduction of the phenoxaphosphino moiety and are to a lesser extent the result of decreased phosphorus basicity.

Catalysis: Activity. Widening the bite angle in the square-planar (diphosphine)Rh(CO)H complex, one of the supposed intermediates in the hydroformylation reaction would certainly accelerate the overall reaction by increasing the concentration of this intermediate complex, as a trans coordination of the diphosphine is energetically more favorable than a cis coordination. If other effects are absent or counterbalance one another (i.e., alkene and CO association/dissociation, hydride and alkyl migration, and hydrogenolysis), then this leads to an increase in hydroformylation activity, as was postulated previously.[4] In the same study an increased rate of alkene coordination for ligands with a wider bite angle was also proposed in order to explain the effect on reaction rate in accord with other studies.[40,41] While these positive effects of widening the bite angle on activity are certainly not ruled out for **1**−**8**, the results indicate that another step in the catalytic cycle becomes rate-limiting. This effect is especially pronounced in the hydroformylation of *trans*-2-octene. The decrease of hydroformylation activity with increased bite angle might be explained by a step later in the catalytic cycle becoming rate limiting. In the trigonal bipyramidal rhodium complex, increasing the bite angle results in increased steric congestion around rhodium especially in the apical position. In addition, with the exception of **2** and **7** an increased bite angle leads to a decreased phosphorus−hydride coupling, which is indicative of approaching a more perfect trigonal bipyramidal structure. This might be an indication that ligands with a larger bite angle lead to less distorted trigonal bipyramidal complexes and thereby to an increased effective steric bulk (Figure 7).

According to this postulation, it is more favorable for complexes of **B** (Scheme 2) with wide bite angle ligands

Scheme 2. β-Hydrogen Elimination vs CO Association

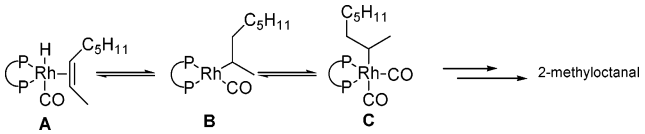

to undergo β-hydrogen elimination (**B** → **A**) than CO association (**B** → **C**), as required for hydroformylation. From the deuterioformylation experiments it can be concluded that isomerization toward internal olefins is faster than isomerization toward the terminal olefin. Also, the rate of isomerization is faster than the rate of CO insertion. Additionally, CO insertion into the branched alkyl rhodium intermediate is slower than CO insertion into the linear alkyl rhodium intermediate; especially when bulky ligands are used, this CO insertion is hampered. Thus, it is reasoned that systems that show a higher rate of isomerization (thus ligands with wide bite angles) show a lower hydroformylation activity. For 1-octene hydroformylation these effects are less pronounced, as differences between the rate of β-hydrogen elimination from the linear alkyl rhodium species are smaller and since CO association to a linear alkyl rhodium intermediate is sterically less demanding.

Another explanation for the bite angle effect on the activity in hydroformylation is found in a decreased rate of alkene insertion. The increased steric congestion around rhodium hampers the olefin from entering the coordination sphere. For internal olefins this effect is stronger than for terminal olefins.

Catalysis: Regioselectivity. Concerning regioselectivity, the series does follow the trend that was observed before;[4] that is, ligands possessing larger bite angles lead to more regioselective systems. It must be noted that the origin of the regioselectivity is different from that reported previously in which the increase in selectivity is attributed to more selective formation of the linear alkyl-rhodium species. In the present study using **1**−**8** the differences in regioselectivity are caused by the differences in rate of β-hydrogen elimination of the branched alkyl intermediate compared to the linear alkyl intermediate, as supported by the deuterioformylation experiments. The branched alkyl intermediate reverts to an olefin complex, but the linear alkyl intermediate is converted directly to the aldehyde.[32] As more linear than branched products are formed for hydroformylation of *trans*-2-octene using **2**−**8**, it can be concluded that most products are formed via in situ generated terminal olefins. The order in the regioselectivities of the different systems is therefore unchanged. It can be concluded that the formation of terminal olefins from internal olefins is faster than the formation of branched aldehydes.

Upon increasing the natural bite angle to 131° with ligand **8**, a decrease in regioselectivity is observed. Although this might be due to possible coordination of the phosphine in the ligand backbone, thereby acting partially as a monophosphine, it is unlikely that this is happening, since at low phosphorus concentrations and under CO pressure the monophosphine would dissociate. A more plausible reason is that systems possessing too large bite angles again lead to less regioselective systems by relatively increasing the rate of β-hydrogen

(39) Bregman, F. R.; Ernsting, J. M.; Müller, F.; Boele, M. D. K.; van der Veen, L. A.; Elsevier, C. J. *J. Organomet. Chem.* **1999**, *592*, 306−311.
(40) Rocha, W. R.; De Almeida, W. B. *Organometallics* **1998**, *17*, 1961−1967.
(41) Thorn, D. L.; Hoffmann, R. *J. Am. Chem. Soc.* **1978**, *100*, 2079−2090.

elimination from the linear alkyl intermediate. An optimum bite angle is found around 120−125°. Previous studies on a dibenzofuran-based diphenylphosphine (4,6-bis(diphenylphosphinodibenzofuran, β_n = 131.1°) also showed a decrease in selectivity compared to similar ligands with a smaller bite angle.[11]

The results with the dibenzophosphole-type ligands **9**, **10**, and **12** show that very subtle changes in either backbone structure or cyclic phosphino moiety can have a tremendous influence on the catalysis results. How these subtle changes influence catalysis is not yet understood. Unfortunately, the preferential formation of the rhodium dimer complex hampers a detailed in situ study.

Conclusions. Within the series of xantphenoxaphos-type ligands no distinct effect of the natural bite angle on the coordination mode of the (**1**−**8**)Rh(CO)$_2$H complexes has been found. Most ligands show ee coordination preferentially, and only for ligands **1**, **2**, and **8** was also ae coordination observed. The decrease of catalytic activity with an increase in natural bite angle is attributed to differences in the rate of β-hydrogen elimination and CO association in the intermediate (**1**−**8**)Rh(CO)(alkyl) complex, and these are mainly determined by steric factors. The differences in selectivity are also attributed to the differences in rate of β-hydrogen elimination, as deuterioformylation experiments have shown that the initial ratio of (linear alkyl)-rhodium intermediate:(branched alkyl)rhodium intermediate is equal when **1**, **5**, and **7** are used. To the best of our knowledge, thixantphenoxaphos (**3**) gives an *unprecedented* high activity with a respectable selectivity in the rhodium-diphosphine-catalyzed hydroformylation of terminal olefins. Noteworthy, though, are the recent results obtained by Stanley et al., who improved existing systems by the addition of water to the reaction medium.[42]

High regioselectivities are observed when the dibenzophosphole-type ligands **9** and **10** are used for the hydroformylation of *trans*-2-octene, which are *unprecedented*. These regioselectivities even supersede the regioselectivities often reported for the hydroformylation of terminal olefins. Despite their moderate 1-octene hydroformylation activity, **9** and **10** still show an acceptable activity in hydroformylation of *trans*-2-octene.

Experimental Section

Computational Details. The molecular mechanics calculations were performed using CAChe WorkSystem version 4.0, on an Apple Power MacIntosh 950, equipped with two CAChe CXP coprocessors. Calculations were carried out similarly to the method described by Casey and Whiteker,[5] using a Rh−P bond length of 2.315 Å. Minimizations were done using the block-diagonal Newton−Raphson method, allowing the structures to converge with a termination criterion of a rms factor of 0.0001 kcal mol^{-1} Å^{-1} or less.

General Procedure. All air- or water-sensitive reactions were performed using standard Schlenk techniques under an atmosphere of purified argon. Toluene was distilled from sodium, THF from sodium/benzophenone, and hexanes from sodium/benzophenone/triglyme. 2-Propanol and dichloromethane were distilled from CaH_2. Chemicals were purchased from Acros Chimica and Aldrich Chemical Co. Benzo[*k*,*l*]xanthene,[43,44] 10,11-dihydrodebenzo[*b*,*f*]oxepine,[45] 9-isopropylidenexanthene,[46] 10-phenylphenoxaphosphine,[47] 2,8-dimethyl-10-chlorophenoxaphosphine,[48] 2,7-di-*tert*-butyl-10,10-dimethylphenoxasilin,[49,50] 2,7-dimethylphenoxathiin,[51] 9-(*tert*-butyldimethylsilyl)phenoxazine,[52] 2,7-di-*tert*-butyl-9,9-dimethyl-4,5-bis(10-phenoxaphosphino)xanthene (**11**),[10,21] and 4,5-bis-(9-dibenzo[*b*,*d*]phospholyl)-2,7-di-*tert*-butyl-9,9-dimethylxanthene (**12**)[10,21] were prepared according to literature procedures. Silica gel 60 (230−400 mesh) purchased from Merck was used for column chromatography. Melting points were determined on a Gallenkamp MFB-595 melting point apparatus in open capillaries and are reported uncorrected. NMR spectra were recorded on a Varian Mercury 300 or Inova 500 spectrometer. ^{31}P and ^{13}C spectra were measured ^{1}H decoupled. TMS was used as a standard for ^{1}H and ^{13}C NMR and 85% of H_3PO_4 in H_2O for ^{31}P NMR. Infrared spectra were recorded on a Nicolet 510 FT-IR spectrophotometer. High-pressure IR spectra were measured using a 50 mL homemade stainless steel autoclave equipped with mechanical stirrer and ZnS windows. Hydroformylation reactions were carried out in a 200 mL homemade stainless steel autoclave. Both high-pressure IR and hydroformylation experiments were conducted at a stirring rate of 800 rpm. The alkene was filtered over neutral activated alumina to remove peroxide impurities. The reactions were stopped by quenching the reaction mixture with tri-*n*-butyl phosphite, cooling on ice, and venting the gases. Synthesis gas (CO/H_2, 1:1, 99.9%) was purchased from Air Liquide. D_2 was purchased from Hoekloos. ^{13}CO (99%) was purchased from Cambridge Isotope Laboratories. Gas chromatographic analyses were run on an Interscience HR GC Mega 2 apparatus (split/splitless injector, J&W Scientific, DB-1 30 m column, film thickness 3.0 mm, carrier gas 70 kPa He, FID detector) equipped with a Hewlett-Packard data system (Chrom-Card) using decane as an internal standard.

4,5-Bis(2,8-dimethyl-10-phenoxaphosphino)-10,11-dihydrodibenzo[*b*,*f*]oxepine (Homoxantphenoxaphos, 1). At 0 °C 1.9 mL of *n*-butyllithium (2.5 M in hexanes, 4.8 mmol) was added to a stirred solution of 380 mg of 10,11-dihydrodibenzo[*b*,*f*]oxepine (1.9 mmol) and 0.73 mL of TMEDA (4.8 mmol) in 10 mL of diethyl ether. The resulting solution was warmed to room temperature overnight. The reaction mixture was cooled to −78 °C, and a solution of 1.25 g of 10-chloro-2,8-dimethylphenoxaphosphine (4.8 mmol) in 10 mL of toluene was added. The reaction mixture was slowly warmed to room temperature overnight. Next the diethyl ether was removed in vacuo, and the mixture was diluted with 30 mL of dichloromethane and hydrolyzed with 10 mL of a 10% aqueous HCl solution. The water layer was removed, and the organic layer was dried over $MgSO_4$. The solvents were removed in vacuo, and the resulting white solid was crystallized from 2-propanol/toluene. Yield: 860 mg of white crystals (68%). Mp: 247−249 °C. ^{31}P{^{1}H} NMR ($CDCl_3$): δ −69.12. ^{1}H NMR ($CDCl_3$): δ 7.67 (d, ^3J(P,H) = 1.5 Hz, 4H), 7.12 (dd, ^3J(H,H) = 8.0 Hz, ^4J(H,H) = 2.0 Hz, 4H), 7.07 (d, ^3J(H,H) = 8.5 Hz, 4H), 7.01 (dd, ^3J(H,H) = 7.0 Hz, ^4J(H,H) = 2.5 Hz, 2H), 6.89 (dd, ^3J(H,H) = 7.0 Hz, ^4J(H,H) = 1.5 Hz, 2H), 6.86 (t, ^3J(H,H) = 7.0 Hz), 3.07 (s, 4H),

(42) Aubrey, D. A.; Bridges, N. N.; Ezell, K.; Stanley, G. G. *J. Am. Chem. Soc.* **2003**, *125*, 11180−11181.
(43) Orchin, M. *J. Am. Chem. Soc.* **1948**, *70*, 495−497.
(44) Yagupsky, G.; Wilkinson, G. *J. Chem. Soc. (A)* **1969**, 725−733.
(45) Hess, B. A., Jr.; Bailey, A. S.; Bartusek, B.; Boekelheide, V. *J. Am. Chem. Soc.* **1969**, *91*, 1665−1672.
(46) McMurry, J. E.; Krepski, L. R. *J. Org. Chem.* **1976**, *41*, 3929−3930.
(47) Schlosser, M. In *Organometallics in Synthesis: A Manual*; Schlosser, M., Ed.; Wiley: Chichester, 1994; p 115.
(48) Freedman, L. D.; Doak, G. O.; Edmisten, J. R. *J. Org. Chem.* **1961**, *26*, 284−285.
(49) Gilman, H.; Trepka, W. J. *J. Org. Chem.* **1961**, *26*, 5202.
(50) Oita, K.; Gilman, H. *J. Am. Chem. Soc.* **1957**, *79*, 339−342.
(51) Suter, C. M.; McKenzie, J. P.; Maxwell, C. E. *J. Am. Chem. Soc.* **1936**, *58*, 717−720.
(52) Antonia, Y.; Barrera, P.; Contreras, O.; Franco, F.; Galeazzi, E.; Garcia, J.; Greenhouse, R.; Guzman, A.; Velarde, E.; Muchowski, J. M. *J. Org. Chem.* **1948**, *54*, 2159−2165.

2.24 (s, 12H). $^{13}C\{^1H\}$ NMR ($CDCl_3$): δ 158.01 (t, 10.9 Hz), 153.23 (s), 135.10 (t, 18.7 Hz), 132.86 (t, 16.6 Hz), 132.68 (s), 132.449 (t, 4.9 Hz), 131.34 (s), 131.02 (s), 123.91 (s), 118.83 (s), 117.24 (s), 32.58 (s), 20.51 (s). Anal. Calcd for $C_{42}H_{34}O_3P_2$: C, 77.77; H, 5.28. Found: C, 77.95; H, 5.40.

4,5-Bis(2,8-dimethyl-10-phenoxaphosphino)-2,7-di-*tert*-butyl-10,10-dimethylphenoxasilin (Sixantphenoxaphos, 2). At 0 °C 3.6 mL of *n*-butyllithium (2.5 M in hexanes, 9.0 mmol) was added to a stirred solution of 1.23 g of 2,7-di-*tert*-butyl-10,10-dimethylphenoxasilin (3.6 mmol) and 1.4 mL of TMEDA (9.3 mmol) in 20 mL of diethyl ether. The resulting solution was warmed to room temperature overnight. The reaction mixture was cooled to −78 °C, and a solution of 2.4 g of 10-chloro-2,8-dimethylphenoxaphosphine (9.1 mmol) in 10 mL of toluene was added. The reaction mixture was slowly warmed to room temperature overnight. Next the diethyl ether was removed in vacuo, and the mixture was diluted with 60 mL of dichloromethane and hydrolyzed with 20 mL of a 10% aqueous HCl solution. The water layer was removed, and the organic layer was dried over $MgSO_4$. The solvents were removed in vacuo, and the resulting yellow-white foam was crystallized from 2-propanol/toluene. Yield: 1.3 g of white crystals (44.4%). Mp: 300−302 °C. $^{31}P\{^1H\}$ NMR ($CDCl_3$): δ −72.09. ^1H NMR ($CDCl_3$): δ 8.06 (s, 4H), 7.42 (d, ^4J(H,H) = 2.5 Hz, 2H), 7.22 (dd, ^3J(H,H) = 8.5 Hz, ^4J(H,H) = 2.0 Hz, 4H), 7.17 (d, ^3J(H,H) = 8.0 Hz, 4H), 7.17 (d, ^4J(H,H) = 2.0 Hz, 2H), 2.39 (s, 12H), 1.20 (s, 18H), 0.49 (s, 6H). $^{13}C\{^1H\}$ NMR ($CDCl_3$): δ 156.41 (t, 11.0 Hz), 151.13 (s), 142.05 (s), 132.57 (m), 131.35 (s), 129.54 (s), 128.41 (s), 128.28 (s), 126.12 (s), 125.42 (vt), 115.70 (s), 114.37 (s), 31.28 (s), 28.24 (s), 17.72 (s), −3.0 (s). Anal. Calcd for $C_{50}H_{52}O_3P_2Si$: C, 75.92; H, 6.63. Found: C, 75.75; H, 6.65.

4,5-Bis(2,8-dimethyl-10-phenoxaphosphino)-2,7-dimethylphenoxathiin (Thixantphenoxaphos, 3). At 0 °C 11.0 mL of *n*-butyllithium (2.5 M in hexanes, 27.6 mmol) was added to a stirred solution of 2.5 g of 2,7-dimethylphenoxathiin (11.0 mmol) and 4.2 mL of TMEDA (27.4 mmol) in 50 mL of diethyl ether. The resulting solution was warmed to room temperature overnight. The reaction mixture was cooled to −78 °C, and a solution of 7.2 g of 10-chloro-2,8-dimethylphenoxaphosphine (27.4 mmol) in 30 mL of toluene was added. The reaction mixture was slowly warmed to room temperature overnight. Next the diethyl ether was removed in vacuo, and the mixture was diluted with 120 mL of dichloromethane and hydrolyzed with 40 mL of a 10% aqueous HCl solution. The water layer was removed, and the organic layer was dried over $MgSO_4$. The solvents were removed in vacuo, and the resulting yellow solid was crystallized from 2-propanol/toluene. Yield: 3.3 g of white crystals (43.5%). Mp: 333−338 °C (dec). $^{31}P\{^1H\}$ NMR ($CDCl_3$): δ −71.28. ^1H NMR ($CDCl_3$): δ 7.77 (bs, 4 H), 7.17 (dd, ^3J(H,H) = 8.4 Hz, ^4J(H,H) = 2.1 Hz, 4H), 7.08 (d, ^3J(H,H) = 8.4 Hz, 4H), 6.78 (bs, 2H), 6.46 (bs, 2H), 2.32 (s, 12H), 2.03 (s, 6H). $^{13}C\{^1H\}$ NMR ($CDCl_3$): δ 153.89 (s), 152.61 (t, 12.2 Hz), 149.86 (s), 135.53 (t, 20.8 Hz), 134.61 (s), 132.93 (t, 4.8 Hz), 131.76 (s), 129.74 (t, 15.8 Hz), 128.37 (s), 120.42 (s), 117.97 (t, 3.6 Hz), 117.67 (s), 20.93 (s). Anal. Calcd for $C_{42}H_{34}O_3P_2S$: C, 74.10; H, 5.03. Found: C, 73.48; H, 4.98.

4,5-Bis(2,8-dimethyl-10-phenoxaphosphino)-9-isopropylidenexanthene (Isopropxantphenoxaphos, 4). At 0 °C 5.8 mL of *n*-butyllithium (2.5 M in hexanes, 14.5 mmol) was added to a stirred solution of 1.3 g of 10-isopropylidenexanthene (6.8 mmol) and 2.25 mL of TMEDA (14.6 mmol) in 30 mL of diethyl ether. The resulting solution was warmed to room temperature overnight. The reaction mixture was cooled to −78 °C, and a solution of 3.8 g of 10-chloro-2,8-dimethylphenoxaphosphine (14.5 mmol) in 10 mL of toluene was added. The reaction mixture was slowly warmed to room temperature overnight. Next the diethyl ether was removed in vacuo, and the mixture was diluted with 60 mL of dichloromethane and hydrolyzed with 20 mL of a 10% aqueous HCl solution. The water layer was removed, and the organic layer was dried over $MgSO_4$. The solvents were removed in vacuo, and the resulting yellow solid was precipitated from 2-propanol/toluene. Yield: 1.5 g of a slightly tanned powder (38.8%). Mp: 333−335 °C (dec). $^{31}P\{^1H\}$ NMR ($CDCl_3$): δ −71.10. ^1H NMR ($CDCl_3$): δ 7.86 (bd, ^3J(P,H) = 8.7 Hz, 4H), 7.22 (dd, ^3J(H,H) = 7.2 Hz, ^4J(H,H) = 2.7 Hz, 2H), 7.17 (dd, ^3J(H,H) = 8.4 Hz, ^4J(H,H) = 2.1 Hz, 4H), 7.11 (d, ^3J(H,H) = 8.1 Hz, 4H), 6.92 (t, ^3J(H,H) = 7.5 Hz, 2H), 6.75 (bdd, ^3J(H,H) = 7.8 Hz, ^4J(H,H) = 1.8 Hz, 2H), 2.33 (s, 12H), 2.00 (s, 6H). Anal. Calcd for $C_{44}H_{36}O_3P_2$: C, 78.33; H, 5.38. Found: C, 78.45; H, 5.53.

4,5-Bis(2,8-dimethyl-10-phenoxaphosphino)-9,9-dimethylxanthene (Xantphenoxaphos, 5). At 0 °C 6 mL of *n*-butyllithium (2.5 M in hexanes, 15 mmol) was added to a stirred solution of 1 g of 9,9-dimethylxanthene (4.8 mmol) and 2.2 mL of TMEDA (15 mmol) in 20 mL of diethyl ether. The resulting solution was warmed to room temperature and stirred overnight. The reaction mixture was cooled to −78 °C, and a solution of 3.9 g of 10-chloro-2,8-dimethylphenoxaphosphine (15 mmol) in 20 mL of toluene was added. The reaction mixture was slowly warmed to room temperature and stirred overnight. Next the diethyl ether was removed in vacuo, and the mixture was diluted with 40 mL of dichloromethane and hydrolyzed with 10 mL of a 10% aqueous HCl solution. The water layer was removed, and the organic layer was dried over $MgSO_4$. The solvents were removed in vacuo, and the resulting yellow-white solid was crystallized from 2-propanol/toluene. Yield: 1.9 g of white crystals (59%). Mp: 328−329 °C. $^{31}P\{^1H\}$ NMR ($CDCl_3$): δ −70.96. ^1H NMR ($CDCl_3$): δ 7.98 (d, ^3J(P,H) = 6.0 Hz, 4 H), 7.29 (dd, ^3J(H,H) = 5.0 Hz, ^4J(H,H) = 1.5 Hz, 4H), 7.18 (dd, ^3J(H,H) = 8.5 Hz, ^4J(H,H) = 2.5 Hz, 4H), 7.11 (d, ^3J(H,H) = 8 Hz, 2H), 6.90 (t, ^3J(H,H) = 8.0 Hz, 2H), 6.75 (bd, ^3J(H,H) = 7.5 Hz, 2H), 2.35 (s, 12H), 1.55 (s, 6H). $^{13}C\{^1H\}$ NMR ($CDCl_3$): δ 154.35 (s), 152.41 (t, 10.56 Hz), 135.77 (t, 21.5 Hz), 132.96 (t, 5.4 Hz), 132.09 (s), 131.74 (s), 130.26 (s), 127.79 (vt, 11.44 Hz), 127.18 (s), 123.76 (s), 118.16 (s), 117.66 (s), 34.58 (s), 32.59 (s), 20.85 (s). Anal. Calcd for $C_{43}H_{36}O_3P_2$: C, 77.93; H, 5.48. Found: C, 77.91; H, 5.54.

6,7-Bis(2,8-dimethyl-10-phenoxaphosphino)benzo[*k,l*]-xanthene (Benzoxantphenoxaphos, 6). At 0 °C 0.8 mL of *n*-butyllithium (2.5 M in hexanes, 2.0 mmol) was added to a stirred solution of 180 mg of benzo[*k,l*]xanthene (0.82 mmol) and 0.31 mL of TMEDA (2 mmol) in 10 mL of diethyl ether. The resulting solution was warmed to room temperature overnight. The reaction mixture was cooled to −78 °C, and a solution of 525 mg of 10-chloro-2,8-dimethylphenoxaphosphine (2.0 mmol) in 5 mL of toluene was added. The reaction mixture was slowly warmed to room temperature overnight. Next the diethyl ether was removed in vacuo, and the mixture was diluted with 40 mL of dichloromethane and hydrolyzed with 10 mL of a 10% aqueous HCl solution. The water layer was removed, and the organic layer was dried over $MgSO_4$. The solvents were removed in vacuo, and the resulting yellow solid was crystallized from 2-propanol/toluene. Yield: 280 mg of yellow crystals (51%). Mp: 308−310 °C. $^{31}P\{^1H\}$ NMR ($CDCl_3$): δ −70.86. ^1H NMR ($CDCl_3$): δ 8.14 (bd, ^3J(H,H) = 6.5 Hz, 2H), 7.94 (bd, ^3J(H,H) = 6.5 Hz, 2H), 7.86 (dd, ^3J(H,H) = 8.0 Hz, ^4J(H,H) = 1.5 Hz, 1H), 7.70 (d, ^3J(H,H) = 7.0 Hz, 1H), 7.50 (d, ^3J(H,H) = 7.5 Hz, 1H), 7.40 (t, ^3J(H,H) = 7.5 Hz, 1H), 7.26−7.2 (m, 5H), 7.17−7.13 (m, 8.0 Hz, 4H), 6.95 (t, 8.0 Hz, 1H), 6.88 (dd, ^3J(H,H) = 8.5 Hz, ^3J(H,H) = 1.5 Hz, 1H), 6.73 (bdd, ^3J(H,H) = 7.5 Hz, ^3J(H,H) = 1.5 Hz, 1H), 2.39 (s, 6H), 2.37 (s, 6H). $^{13}C\{^1H\}$ NMR ($CDCl_3$): δ 155.59 (s), 154.98 (s), 154.41 (t, 10.9 Hz), 136.58 (vt), 136.56 (s), 136.05 (vt), 134.81 (s), 134.06 (m), 132.87 (s), 132.55 (s), 131.76 (s), 129.56 (s), 129.18 (s), 128.25 (s), 126.65 (s), 125.03 (s), 124.81 (s), 122.17 (s), 121.72 (s), 121.63 (s), 119.40 (s), 119.15 (s), 118.96 (t, 2.7 Hz), 118.48 (s), 118.46 (s), 118.43 (s), 118.34 (s), 116.28 (s), 20.83 (s), 20.80 (s). Anal. Calcd for $C_{44}H_{32}O_3P_2$: C, 78.80; H, 4.81. Found: C, 79.52; H, 5.01.

4,5-Bis(2,8-dimethyl-10-phenoxaphosphino)phenoxazine (Nixantphenoxaphos, 7). At 0 °C 13.8 mL of *n*-

butyllithium (2.5 M in hexanes, 34.5 mmol) was added to a stirred solution of 4.0 g of 9-(*tert*-butyldimethylsilyl)phenoxazine (13.5 mmol) and 5.2 mL of TMEDA (34.5 mmol) in 200 mL of diethyl ether. The resulting solution was warmed to room temperature overnight. The reaction mixture was cooled to −78 °C, and a solution of 9.1 g of 10-chloro-2,8-dimethylphenoxaphosphine (34.5 mmol) in 60 mL of toluene was added. The reaction mixture was slowly warmed to room temperature overnight. Next the diethyl ether was removed in vacuo, and the mixture was diluted with 120 mL of dichloromethane and hydrolyzed with 40 mL of a 10% aqueous HCl solution. The water layer was removed, and the organic layer was dried over $MgSO_4$. The solvents were removed in vacuo, and the resulting brown paste was dissolved in 100 mL of THF. *n*-$(Bu)_4NF{\cdot}3H_2O$ (8.62 g, 33 mmol) was added, and the reaction mixture was stirred for 2 days at room temperature. Then 50 mL of brine and 200 mL of dichloromethane were added. The water layer was removed, and the organic layer was dried on $MgSO_4$. The solvents were removed in vacuo, and the resulting yellow solid was crystallized from dichloromethane/ethanol. Yield: 2.6 g of brown-yellow microcrystals (30%). Mp: 276 °C (dec). $^{31}P\{^1H\}$ NMR ($CDCl_3$): δ −70.71. ^1H NMR ($CDCl_3$): δ 7.98 (d, $^3J(P,H) = 9.5$ Hz, 4H), 7.20 (dd, $^3J(H,H) = 8.5$ Hz, $^4J(H,H) = 1.9$ Hz, 4H), 7.06 (d, $^3J(H,H) = 8.5$ Hz, 4H), 6.41 (t, $^3J(H,H) = 7.5$ Hz, 2H), 6.18 (d, $^3J(H,H) = 7.5$ Hz, 2H), 5.93 (dd, $^3J(H,H) = 7.5$ Hz, $^4J(H,H) = 1.8$ Hz, 2H), 4.76 (bs, 1H), 2.37 (s, 12H). $^{13}C\{^1H\}$ NMR ($CDCl_3$): δ = 155.38 (s), 136.63 (vt, 21.9 Hz), 135.01 (s), 133.87 (t, 5.5 Hz), 133.67(t, 2.4 Hz), 132.56 (s), 131.91 (s), 125.01 (s), 124.82 (s), 118.67 (s), 118.25 (s), 114.57 (s), 20.83 (s), 20.82 (s). Anal. Calcd. for $C_{40}H_{31}NO_3P_2$: C, 75.58; H, 4.92; N, 2.20. Found: C, 75.14; H, 4.89; N, 2.31.

4,5-Bis(2,8-dimethyl-10-phenoxaphosphino)-10-phenylphenoxaphosphine (Phosxantphenoxaphos, 8). At room temperature 23 mL of phenyllithium (1.8 M in hexanes, 41.4 mmol) was added to a stirred solution of 1.5 g of 10-phenylphenoxaphosphine (5.4 mmol) and 6.24 mL of TMEDA (40.7 mmol) in 30 mL of diethyl ether. The dark brown reaction mixture was heated at reflux temperature for 2 days. Then the reaction mixture was cooled to −78 °C, and a solution of 10.7 g of 10-chloro-2,8-dimethylphenoxaphosphine (40.7 mmol) in 80 mL of toluene was added. The reaction mixture was slowly warmed to room temperature overnight. Next the diethyl ether was removed in vacuo, and the mixture was diluted with 120 mL of dichloromethane and hydrolyzed with 40 mL of a 10% aqueous HCl solution. The water layer was removed, and the organic layer was dried over $MgSO_4$. The resulting solid was filtered through silica gel (eluent: toluene). The solvent was removed in vacuo, and the resulting white solid was purified by several washings with boiling hexanes. Yield: 1.5 g of a white powder (37.9%). Alternatively, crystals can be obtained from dichloromethane/ethanol. Mp: 256−258 °C. $^{31}P\{^1H\}$ NMR ($CDCl_3$): δ −53.08, −70.38 (ratio 1:2). ^1H NMR (CD_2Cl_2): δ 7.93 (m, 2H), 7.84 (m, 2H), 7.40 (ddd, $^4J(P,H) = 10.5$ Hz, $^3J(H,H) = 6.3$ Hz, $^4J(H,H) = 2.4$ Hz, 2H), 7.23 (m, 5H), 7.14 (d, $^3J(H,H) = 7.2$ Hz, 4H), 7.09 (m, 4H), 6.96 (m, 4H), 2.34 (s, 6H), 2.32 (s, 6H). $^{13}C\{^1H\}$ NMR (CD_2Cl_2): δ 157.05 (t, 10.3 Hz), 154.18 (d, 6.8 Hz), 140.17 (d, 21.2 Hz), 136.24 (d, 35.7 Hz), 136.02 (s), 135.74 (t, 20.61 Hz), 135.59 (t, 19.9 Hz), 133.52 (dt, 12.5 Hz, 5.6 Hz), 132.63 (s), 132.46 (s), 132.36 (s), 130.54 (vt, 17.1 Hz), 129.46 (s), 129.03 (d, 6.9 Hz), 124.94 (d, 11.7 Hz), 119.97 (d, 4.8 Hz), 118.29 (t, 2.8 Hz), 118.01 (d, 11.1 Hz), 20.95 (s), 20.90 (s). Anal. Calcd for $C_{46}H_{35}O_3P_3$: C, 75.82; H, 4.84. Found: C, 75.89; H, 4.74.

4,5-Bis(9-dibenzo[*b,d*]phospholyl)-2,7-dimethylphenoxathiin (DBP−Thixantphos, 9). At 0 °C 4.4 mL of *n*-butyllithium (2.5 M in hexanes, 11.0 mmol) was added to a stirred solution of 1.1 g of 2,7-dimethylphenoxathiin (4.7 mmol) and 1.7 mL of TMEDA (27.4 mmol) in 25 mL of diethyl ether. The resulting solution was warmed to room temperature overnight. The reaction mixture was cooled to −78 °C, and a solution of 2.4 g of 9-chlorodibenzo[*b,d*]phosphole (11.0 mmol) in 10 mL of toluene was added. The reaction mixture was slowly warmed to room temperature overnight. Next the diethyl ether was removed in vacuo, and the mixture was diluted with 100 mL of dichloromethane and hydrolyzed with 30 mL of a 10% aqueous HCl solution. The water layer was removed, and the organic layer was dried over $MgSO_4$. The solvents were removed in vacuo, and the resulting yellow solid was crystallized from 2-propanol/toluene. Yield: 1.3 g of colorless crystals (47%). Mp: 345 °C (dec). $^{31}P\{^1H\}$ NMR (THF-d_8): δ −19.78. ^1H NMR (THF-d_8): δ 8.1 (dd, $^3J(H,H) = 7.5$ Hz, $^4J(H,H) = 1.6$ Hz, 4H), 8.09 (d, $^3J(H,H) = 7.5$ Hz, 4H), 7.45 (t, $^3J(H,H) = 7.5$ Hz, 4H), 7.36 (t, $^3J(H,H) = 7.2$ Hz, 4H), 6.95 (bs, 2H), 6.32 (bs, 2H), 1.99 (s, 6H). $^{13}C\{^1H\}$ NMR ($CDCl_3$): δ 153.38 (t, 11.6 Hz), 143.91 (s), 142.31 (t, 2.3 Hz), 134.53 (s), 131.36 (t, 6.2 Hz), 129.99 (s), 129.03 (s), 128.54 (s), 128.25 (s), 127.38 (t, 3.1 Hz), 126.24 (vt, 13.1 Hz), 121.38 (s), 20.41 (s). Anal. Calcd for $C_{38}H_{26}O_3P_2S$: C, 77.01; H, 4.42. Found: C, 76.85; H, 4.37.

4,5-Bis(9-dibenzo[*b,d*]phospholyl)phenoxazine (DBP−Nixantphos, 10). At 0 °C 6.8 mL of *n*-butyllithium (2.5 M in hexanes, 16.9 mmol) was added to a stirred solution of 2.2 g of 9-(*tert*-butyldimethylsilyl)phenoxazine (7.4 mmol) and 2.6 mL of TMEDA (16.9 mmol) in 100 mL of diethyl ether. The resulting solution was warmed to room temperature overnight. The reaction mixture was cooled to −78 °C, and a solution 3.7 g of 9-chlorodibenzo[*b,d*]phosphole (16.9 mmol) in 30 mL of toluene was added. The reaction mixture was slowly warmed to room temperature overnight. Next the diethyl ether was removed in vacuo, and the mixture was diluted with 100 mL of dichloromethane and hydrolyzed with 30 mL of a 10% aqueous HCl solution. The water layer was removed, and the organic layer was dried over $MgSO_4$. The solvents were removed in vacuo, and the resulting brown paste was dissolved in 100 mL of THF. *n*-$(Bu)_4NF{\cdot}3H_2O$ (4.22 g, 16.2 mmol) was added, and the reaction mixture was stirred for 2 days at room temperature. Then 30 mL of brine and 100 mL of dichloromethane were added. The water layer was removed, and the organic layer was dried on $MgSO_4$. The solvents were removed in vacuo, and the resulting yellow solid was crystallized from dichloromethane/ethanol. Yield: 1.6 g of yellow crystals (43%). Mp: 268 °C (dec). $^{31}P\{^1H\}$ NMR (THF-d_8): δ −20.52. ^1H NMR (THF-d_8): δ 8.22 (bdd, $^3J(H,H) = 7.2$ Hz, $^4J(H,H) = 1.2$ Hz, 4H), 7.99 (d, $^3J(H,H) = 7.5$ Hz, 4H), 7.44 (t, $^3J(H,H) = 7.2$ Hz, 4H), 7.37 (t, $^3J(H,H) = 7.2$ Hz, 4H), 6.41 (td, $^3J(H,H) = 7.5$ Hz, $^3J(P,H) = 1.2$ Hz, 2H), 6.30 (d, $^3J(H,H) = 7.8$ Hz, 2H), 5.93 (bdd, $^3J(H,H) = 7.5$ Hz, $^4J(H,H) = 1.2$ Hz, 2H), 5.5 (s, 1H). $^{13}C\{^1H\}$ NMR (THF-d_8): δ 147.58 (t, 10.8 Hz), 144.98 (s), 143.11 (s), 133.92 (s), 132.45 (t, 13.1 Hz), 129.45 (s), 128.24 (s), 125.04 (s), 124.63 (vt, 12.6 Hz), 122.78 (s), 122.34 (s), 115.03 (s). Anal. Calcd for $C_{46}H_{35}O_3P_3$: C, 78.97; H, 4.23; N, 2.56. Found: C, 79.11; H, 4.33; N, 2.41.

Hydroformylation. In a typical experiment the autoclave was charged with a 8.5 mL solution of $Rh(CO)_2(acac)$ and 5 equiv of ligand in toluene. After purging the solution three times with CO/H_2 (1:1), the reactor was brought to 16 bar of CO/H_2. Next the autoclave was heated to 80 °C. After 1 h at 80 °C the substrate and internal standard were charged to the reaction mixture by overpressure of CO/H_2 (1:1).

Deuterioformylation. In a typical experiment the autoclave was charged with a 8.5 mL solution of $Rh(CO)_2(acac)$ and 5 equiv of ligand in toluene. After purging the solution three times with D_2, the reactor was brought to 8 bar of D_2 and further pressurized to 16 bar with CO. Next the autoclave was heated to 80 °C. After 1 h at 80 °C the substrate was charged to the reaction mixture by overpressure of CO. Samples of the crude reaction mixture were analyzed by GC. Thereafter the reaction mixture was distilled to separate the hexenes from the aldehydes. Deuterium contents were determined by ^2H NMR; data identical to the data reported by Casey et al. were obtained.[32]

High-Pressure NMR Experiments. In a typical experiment a solution of 5.2 mg of $Rh(CO)_2(acac)$ (20 μmol) and 1.1 equiv of ligand in 1.5 mL of toluene-d_8 was pressurized to 16 bar of CO/H_2. In the NMR spectrometer the tube was heated to 40 °C until complete formation of the rhodium hydride was observed. NMR spectra at different temperatures were recorded.

High-Pressure FT-IR Experiments. In a typical experiment the high-pressure IR autoclave was charged with a solution of 4 mg of $Rh(CO)_2(acac)$ and 1.1 equiv of ligand in 15 mL of cyclohexane. The autoclave was purged three times with 10 bar CO/H_2 (1:1), pressurized to 16 bar, and heated to 40 °C. Catalyst formation was monitored in time. Hydride−deuterium exchange was carried out by cooling the autoclave to room temperature, venting the gases, and purging the solution three times with 5 bar of D_2. Next the autoclave was pressurized to 5 bar D_2, and finally the autoclave was brought to 10 bar by further pressurization with CO.

Acknowledgment. Financial support from Celanese Chemicals Europe, Gmbh, Germany, is gratefully acknowledged.

OM034012F